

Plasmoid-Induced Pull Reconnection Experiments in University of Tokyo Spherical Tokamak^{*})

Takenori G WATANABE, Yasushi ONO, Takuma YAMADA¹⁾, Shuji KAMIO²⁾, Qinghong CAO³⁾, Hiroto IITAGAKI, Koichiro TAKEMURA, Kotaro YAMASAKI³⁾, Koji ISHIGUCHI⁴⁾ and Michiaki INOMOTO

Graduate School of Frontier Sciences, The University of Tokyo, Kashiwa 277-8561, Japan

¹⁾*Faculty of Arts and Science, Kyushu University, Fukuoka 819-0395, Japan*

²⁾*National Institute for Fusion Science, 322-6 Oroshi-cho, Toki 509-5292, Japan*

³⁾*Graduate School of Engineering, The University of Tokyo, Bunkyo 113-8656, Japan*

⁴⁾*The Open University of Japan, Mihama 261-8586, Japan*

(Received 7 December 2012 / Accepted 26 July 2013)

Magnetic energy injection through pull magnetic reconnection has been studied in the University of Tokyo Spherical Tokamak (UTST) using external poloidal field coils. Under constant plasma inflow, the magnetic energy of the produced ST increases as the guide field B_t is increased from zero to the optimized value B_{t0} , while it decreases after B_t exceeds B_{t0} . The pull reconnection process was often accompanied by the formation of plasmoids around the X-point. The reconnection rate was found to change with time, depending on the formation of plasmoids and the magnetic energy injection. Plasmoids enhance the reconnection rate.

© 2013 The Japan Society of Plasma Science and Nuclear Fusion Research

Keywords: magnetic reconnection, helicity injection, plasmoid, current sheet, spherical tokamak, toroidal magnetic field

DOI: 10.1585/pfr.8.2401148

1. Introduction

Startup of spherical tokamak (ST) plasmas by external coil system is an important subject for a low-aspect-ratio ST with a narrow center solenoid space. Helicity (magnetic energy) injection is directly related with the external coil startup, and its relationship has been theoretically and experimentally studied in the University of Tokyo Spherical Tokamak (UTST) experiment. In this helicity injection, two pairs of poloidal field (PF) coils generate poloidal fluxes that serve as helicity sources. Each source was connected to a helicity sink (the ST) through the pull type reconnection regions. We have already reported a mechanism for this helicity injection by using eigenvalues [1].

However, we have not solved whether the helicity injection increases by increasing the guide field and whether the plasmoids formation increases the helicity injection. There are theoretical reports on the relationship between the reconnection and plasmoids [2, 3], but almost no experimental reports have been published.

For the first time, we have measured and finally optimized the helicity injection as a function of the guide field and studied its relationship with the plasmoid formation process during the pull reconnection in UTST. This study addresses how the guide field is optimized for the ST startup and analyzes the interrelation between pull re-

connection, plasmoids and helicity injection.

2. The UTST Device

The important feature of the UTST is that, to demonstrate startup by plasma merging in a reactor relevant situation all the poloidal field coils are located outside the vacuum vessel. The vacuum vessel has an axial (Z) length of about 2 m and a major radius (R) of about 0.7 m [4, 5]. Figure 1 shows the cross-sectional view of the UTST device. Two-dimensional magnetic probe arrays are shown in the left side. The pickup coil array in the upper region of the vacuum vessel ($0.35 \text{ m} \leq Z \leq 0.95 \text{ m}$) has 64 channels of B_z coils and 64 channels of B_t coils. The array in the middle region ($-0.23 \text{ m} \leq Z \leq 0.23 \text{ m}$) has 81 channels of B_z coils and 81 channels of B_t coils. All 290 channels are simultaneously sampled with digitizers at a sampling frequency of 1.0 MHz.

On the basis of the measured 2-D magnetic field profile, the poloidal magnetic flux Ψ is calculated from B_z by $\Psi = 2\pi \int B_z R dR$. The right pannel of Fig. 1 shows the coil flux connected to an ST through magnetic field lines. In the helicity injection experiments, a pair of PF #1 coils was used to form an X-point and coil fluxes, which work as helicity sources. In this paper, the ST plasma was generated by induction of center solenoid coil without merging which allowed us to clearly estimate the effect of magnetic energy injection through pull magnetic reconnection. The plasma current of this ST plasma is lower than that of the

author's e-mail: watanabe@ts.t.u-tokyo.ac.jp

^{*}) This article is based on the presentation at the 22nd International Toki Conference (ITC22).

ST plasma with the merging operation.

Figure 2 shows the time evolution of the poloidal magnetic flux contour. As shown at 400 μ s in Fig. 2, the ST plasma and coil fluxes on both sides of ST plasma were generated. After the ST was connected with the coil fluxes through the X-point at 600 μ s. The pull reconnection started in the connection region between the ST and coil flux, transforming the common flux into a private flux to form a long thin current sheet. The pull mode magnetic reconnection means that the poloidal flux in the common flux is pulled back toward the X-point. At 800 μ s and 1000 μ s, Fig. 2 shows that the plasmoids grew intermittently in the current sheet and moved toward the central ST plasma at around $Z = 0.45$ m. Magnetic helicity injection occurred

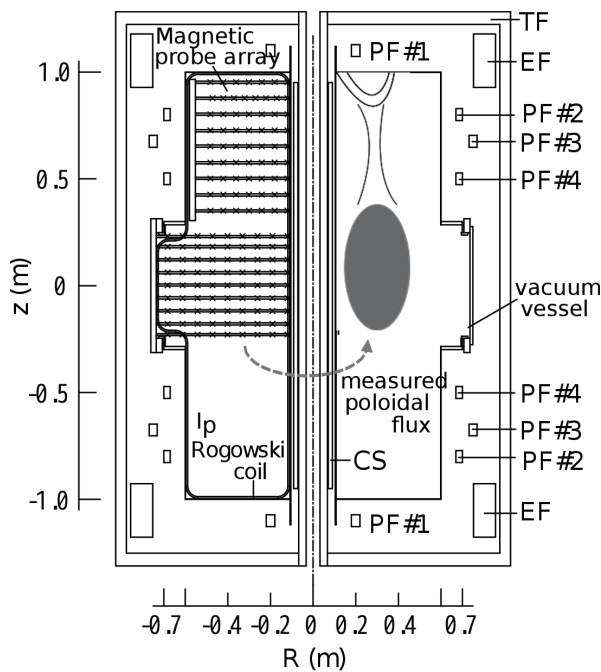


Fig. 1 Cross-sectional view of the UTST device. Two-dimensional magnetic probe arrays are located on the left side. The coil flux is connected with an ST through magnetic field lines.

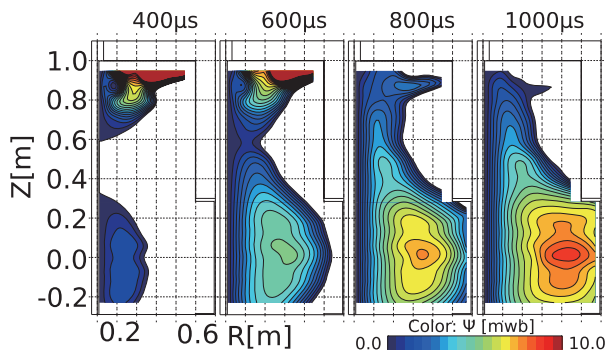


Fig. 2 Time evolution of poloidal magnetic flux contours during the pull reconnection of ST formation.

from the helicity source (the coil flux) into the helicity sink (the ST plasma). The helicity injection was observed around the connection region between the coil flux and the ST plasma. The pull magnetic reconnection was measured by two-dimensional magnetic probe arrays.

3. Experimental Results

We investigated the generation and growth of the plasmoids and the effect of the helicity injection under various conditions, e.g., changing the guide field (the toroidal magnetic field). We calculated the poloidal magnetic energy under the assumption of toroidal symmetry from measured 2-D magnetic field profiles. The poloidal magnetic energy W_{B_p} was obtained by integrating the poloidal magnetic pressure in the region ($0.0 \text{ m} \leq Z \leq 0.6 \text{ m}$), which an ST generated only by ohmic heating without another helicity injection from external poloidal coils.

$$B_r = -\frac{1}{2\pi r} \frac{\partial \Psi}{\partial z}, \quad (1)$$

$$W_{B_p} = \int_V P dv \quad (2)$$

$$= \frac{1}{2\mu_0} \int_V B_p^2 dv. \quad (3)$$

Figure 3 shows the maximum values of the poloidal magnetic energy in seven cases of toroidal magnetic fields. The poloidal magnetic energy of the ST increased as the toroidal magnetic field B_t is increased to $B_t = 0.282$ T, and then decreased when B_t exceeded 0.282 T. In a case that an ST plasma is generated only by CS coil induction, a higher toroidal field increases the magnetic energy up to a critical value, but the field decreases above the critical value. The optimized guide field for the magnetic energy of produced ST was around 0.282 T, which indicates that the helicity was most effectively injected under the proper toroidal magnetic field. This result is similar to those obtained using other devices [6, 7].

To investigate its mechanism, we compared the lowest guide field case {(a) $B_t = 0.220$ T}, the optimized case

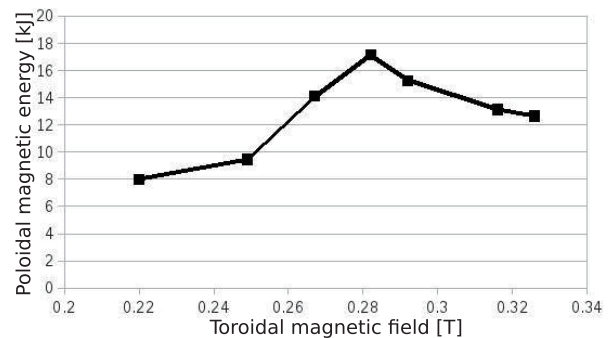


Fig. 3 Maximum values of poloidal magnetic energy of ST plasma formed by CS coil induction as a function of the toroidal magnetic field at $Z = 0.00$ m and $R = 0.25$ m.

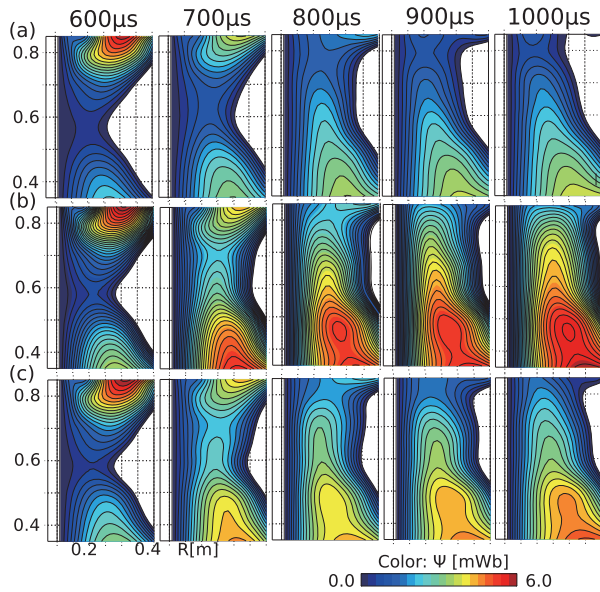


Fig. 4 Time evolutions of poloidal magnetic flux contours in three cases of guide toroidal fields, (a) $B_t = 0.220$ T (b) $B_t = 0.282$ T and (c) $B_t = 0.326$ T.

{ (b) $B_t = 0.282$ T} and the highest case {(c) $B_t = 0.326$ T}. Figure 4 shows time evolutions of poloidal magnetic flux contours for the three cases. In all three cases, the length of the sheet became much longer than its thickness shortly after the helicity source (the poloidal coils) was connected with the helicity sink (the ST plasma) through the X-point. After this time, plasmoids were observed, especially around $Z = 0.45$ m at $800 \mu\text{s}$ in Figs. 4 (b) and 4 (c). The largest plasmoids were observed in 4 (b). This fact suggests that the larger plasmoids are generated under the proper toroidal magnetic field. Under the present condition, both of magnetic helicity of plasmoid and the magnetic energy of produced ST are related, having the optimized condition around $B_t \sim 0.282$ T. This fact suggests that the plasmoid helicity is closely related to the helicity injection into the ST. Below the optimized value, the higher guide field improves helicity injection and the ST plasma, whereas the reconnection rate is decreased [8, 9].

Fluctuations of 1% - 2% of the total poloidal magnetic energy were generated during the time that the plasmoids were observed, leading us to perform detailed measurement in the area around the reconnection. Figure 5 (a) shows the poloidal magnetic flux contours in Fig. 4 (c). The red lines show selected values of the poloidal magnetic flux (2.0, 2.1, 2.2, 2.3, and 2.4 mWb) that were near the X-point at these times. The red lines moved at different speeds at different times; in other words, the reconnection rate drastically changed within a very short period.

Figure 5 (b) shows the time evolutions of the poloidal magnetic energy of the ST plasma, the poloidal magnetic flux at the X-point, and the peak poloidal magnetic fluxes (i.e. Ψ at the point $B_z = 0$) at $Z = 0.60$ m, 0.65 m, and 0.70 m. The rate of decline of the poloidal magnetic flux at

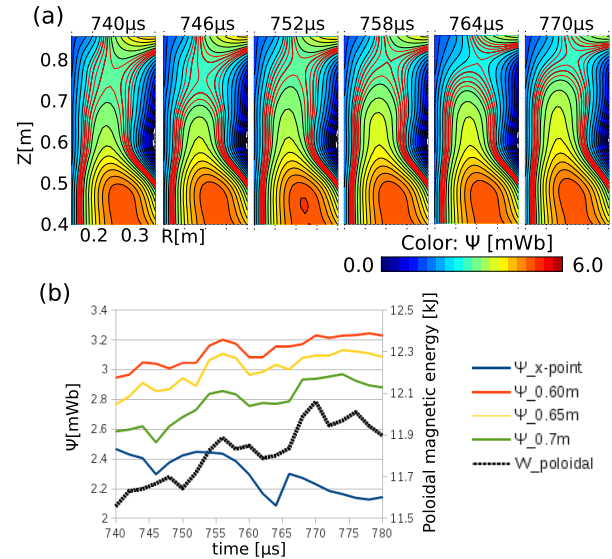


Fig. 5 (a) Poloidal magnetic flux contours in the strongest guide field case ($B_t = 0.326$ T). (b) Time evolutions of the poloidal magnetic energy of the ST plasma, the poloidal magnetic flux at the X-point, and the peak poloidal magnetic fluxes at $Z = 0.60$ m, 0.65 m, and 0.70 m.

the X-point passed through local minimum values at $744 \mu\text{s}$ and $760 \mu\text{s}$. This means that the reconnection rate became a local maximum at those times. The downstream area of the reconnection was affected by the rapid change in the reconnection rate, which makes helicity injection rate nonsteady. As shown in Fig. 5 (b), the poloidal magnetic energy and the peak poloidal magnetic flux increased shortly after the time at which the reconnection rate became a maximum. It was the same for the poloidal magnetic flux at each point. Plasmoids were emitted from the X-point to the ST plasma after the reconnection rate peaked. These results indicate that plasmoids enhance the reconnection rate.

4. Summary

Plasmoid size and the efficiency of helicity injection are maximized when the strength of the toroidal magnetic field is at the optimized value. The optimized guide field enables us to make most efficient helicity as well as magnetic energy. The formation of plasmoids causes the reconnection rate to be drastically intermittent. When plasmoids were ejected to the downstream, the reconnection rate became a maximum. Nonsteady fast reconnection is composed of the formation and ejection of plasmoids, which causes nonsteady evolution of magnetic energy. This makes the helicity injection rate and the growth of an ST plasma nonsteady.

In future, new magnetic coils for measuring small plasmoids will be inserted to conclude how the pull reconnection affects the helicity injection.

Acknowledgment

This work was supported in partial by Grants-in-Aid for Scientific Research (KAKENHI) 22246119, 22686085, and 22656208, and JSPS Core-to-Core Program 22001.

- [1] T.G. Watanabe *et al.*, Plasma Fusion Res. **6**, 1202131 (2011).
- [2] R. Samtaney *et al.*, Phys. Rev. Lett. **103**, 105004 (2009).
- [3] K. Shibata and S. Tanuma, Earth, Planets and Space **53**, 473 (2001).
- [4] T. Yamada *et al.*, Plasma Fusion Res. **5**, S2100 (2010).
- [5] R. Imazawa *et al.*, IEEJ Trans. FM **130**, 4 (2010).
- [6] R. Raman *et al.*, Phys. Plasmas **18**, 092504 (2011).
- [7] A.J. Redd *et al.*, Phys. Plasmas **15**, 092504 (2011).
- [8] Y. Ono, A. Morita, M. Katsurai and M. Yamada, Phys. Fluids B **5**, 3691 (1993).
- [9] M. Yamada, Phys. Plasmas **14**, 058102 (2007).